


Research Article

Trajectory Similarity Matching and Remaining Useful Life Prediction Based on Dynamic Time Warping

Lin Huang , Li Gong, Yutao Chen, Dongliang Li, and Guoqing Zhu 

Navy University of Engineering, Wuhan 430033, China

Correspondence should be addressed to Guoqing Zhu; zhuguoqing1983@126.com

Received 9 September 2022; Revised 3 October 2022; Accepted 8 October 2022; Published 22 October 2022

Academic Editor: Junwei Ma

Copyright © 2022 Lin Huang et al. This is an open access article distributed under the Creative Commons Attribution License, which permits unrestricted use, distribution, and reproduction in any medium, provided the original work is properly cited.

Remaining useful life prediction based on trajectory similarity is a typical example of instance-based learning. Hence, trajectory similarity prediction based on Euclidean distance has the problems of matching and low prediction accuracy. Therefore, an engine remaining useful life (RUL) prediction method based on dynamic time warping (DTW) is proposed. First, aiming at the problem of engine structure complexity and multiple monitoring parameters, the principal component analysis is used to reduce the dimension of multisensor signals. Then, the system performance degradation trajectory is extracted based on kernel regression. After obtaining the degradation trajectory database, the similarity matching of the degradation trajectory is carried out based on DTW. After finding the best matching curve, the RUL can be predicted. Finally, the proposed method is verified by the public aeroengine simulation dataset of NASA, and compared with several representatives and high-precision literature methods based on the same dataset, which verifies the effectiveness of the method.

1. Introduction

In recent years, prognostics and health management (PHM) has attracted progressively more attention in academic and industrial circles. By transforming the conventional reliability-centered maintenance into state-based maintenance, PHM plays a significant role in lowering production cost, improving availability, and providing safety guarantees. Predicting the RUL is a key task in PHM and has become a rapidly growing research focus. It involves a variety of techniques and algorithms in many research fields, such as reliability engineering, time-series modeling, and artificial intelligence [1]. For RUL prediction, an increasing number of methods have been developed, which can be generally divided into model-based and data-driven methods [2].

The model-based prediction methods need to deeply analyze the performance degradation process and physical failure mechanism according to the domain knowledge, and establish a physical failure model to predict the failure time of the equipment [3]. Typical physics-based methods include “Particle Filter” [4, 5], “Wiener model” [6], and “Weibull Distribution” [7]. For example, Wang et al. [4] proposed a

probabilistic model-based approach for machinery condition prognosis based on particle filter in the machinery degradation process and ran an experimental run-to-failure bearing test in a wind turbine. Yu et al. [8] developed a nonlinear-drift-driven Wiener process model considering three sources of variability for the RUL prediction of degrading systems. Moulahi and Ben Hmida [9] proposed a model using the thick-tailed distributions called scale-mixture normal and developed an expectation-maximum algorithm to estimate the model parameters.

The establishment of the physical failure model usually requires an in-depth analysis of the failure mechanism and comprehensive consideration of the physical, chemical, pneumatic, and thermodynamic processes of components, which restricts their generalization [10]. Therefore, the model-based prediction methods are generally only applicable to the prediction of the RUL of component-level equipment. In contrast, data-driven methods only need historical data to learn and predict equipment status, which do not require much domain knowledge [11], and draw a growing number of attentions from researchers. At present, frequently used data-driven methods include “Support

Vector Machine” [12, 13], “Hidden Markov Model” [14], “Relevant Vector Machine” [15], “Gaussian process regression” [16], ensemble prediction technique [17, 18], “Data Mining” [19], and different types of “Deep Neural Network” [20, 21]. These data-driven methods have been widely used since they are put forward. It should be noted that digital twin-driven RUL prediction has rapidly developed in recent years [22, 23]. For example, Meraghni et al. [24] constructed a data-driven digital twin, integrated the physical knowledge of the system, and established an ensemble RUL prediction system. Xiong et al. [25] studied the aeroengine predictive maintenance framework driven by digital twin and developed the implicit digital twin model to improve the effect of predictive engine maintenance.

Among the numerous data-driven methods, the degradation of a system can be described with relatively simple hypotheses or constructed knowledge, which are, therefore, applicable to simple systems or isolated components [26]. Complex systems, however, contain numerous components, and there is little knowledge about their modes or failure mechanisms. Existing RUL models are rarely applied successfully in complex systems. For instance, machine tools, wind turbine generators, and aircraft engines are composed of multiple components, which can cause various failures under the effect of wear and even lead to system degradation [27].

One way to solve the above problem is to use the instance-based learning method. The instance-based learning algorithm [28] is an effective method to extract system features and offers a solution to build a system model based on massive historical data. Past studies on instance-based learning were mainly focused on fault diagnosis but rarely concerned system degradation data to evaluate the similarity of examples in the prediction [29]. Wang et al. [30] introduced an instance-based RUL prediction method called trajectory similarity-based prediction (TSBP). At present, the Euclidean distance is directly employed for trajectory similarity comparison in RUL prediction based on TSBP. In practice, however, it is difficult to implement comparative analysis of the degradation trajectory directly using Euclidean distance since each machine has a different life in the system’s historical database, and each engine has a different operation time and degrades at a different speed in the test data. Therefore, dimension reduction methods have been proposed for degradation trajectory issue, including the “principal component analysis (PCA)” [31], “linear discriminant analysis (LDA)” [32], “locally linear embedding (LLE)” [33], and other improved methods combined with distance for dimension reduction. For example, Liu et al. [31] developed a global surrogate model based on the PCA and Kriging model called PCA-K for efficient uncertainty propagation of dynamic systems in the considered time interval. Huang et al. used LDA to obtain the optimal projection vector by combining it with Lagrangian distance. Yonghe et al. [33] proposed an improved Euclidean distance by the LLE method to obtain the best feature with separability in the new feature space.

In addition to the problem of dimension reduction, another important issue is the matching of degradation

trajectory. Wang [34] introduced a minimum Euclidean distance method with time delay and a Euclidean distance method with a degradation factor. Both methods considered the influence of delay and degradation speed to some extent, but it remained difficult to compare and analyze the degradation trajectory with these methods because the life in the test data varied. Zhang et al. [35] employed the Relief algorithm and PCA to extract the low-dimensional orthogonal multivariate degradation characteristics of the system to perform the RUL prediction. Zhou et al. [36] presented a reduced dimension kernel recurrence least-squares algorithm to process the multidimensional sensor data and combined the method with the hidden Markov models for the remaining life prediction of multiple sensors.

However, the methods mentioned above do not consider the following two issues. First, the performance of a system starts to degrade randomly or because of some unknown external factors. The start of performance degradation varies from sample to sample. Second, system performance degrades at varying speeds. In other words, the degradation curve is consistently monotonic but develops at different speeds. Therefore, it is not satisfactory to simply measure the similarity based on the Euclidean distance. To solve the above problems, we propose a matching method based on DTW. DTW was first applied in speech recognition and online signature verification [37] and can identify the unequal time-series similarity by using the characteristic matching [38], which is suitable for trajectory matching of varying speeds and different starting points and has been widely used in the following areas including automatic hand gesture recognition [39], speech recognition [40], road anomaly detection [41], and mechanical fault diagnostics [42].

In the present work, we aim to tackle the challenges mentioned above and focus on the prediction of RUL based on trajectory similarity matching. The main contributions presented in this paper are summarized as follows:

- (1) A novel RUL prediction method is proposed, which enables the engine RUL prediction based on extraction and matching of degradation trajectory. In particular, we propose a method to measure the similarity between system performance degradation trajectories based on DTW, which enables the measurement of similarity between the trajectories at different lengths of a time series and at different degradation speeds.
- (2) The specific technical process of the RUL prediction method based on DTW is designed. The principal component analysis is first carried out for dimension and noise reduction. Then, the kernel regression is employed for the smoothing and further noise reduction of degradation trajectories. Subsequently, we propose a Euclidean distance measurement method derived from the likelihood function in order to improve calculation accuracy. At last, we calculate the similarity based on the DTW method and predict RUL on this basis.

- (3) The effectiveness of the proposed method is validated based on the aircraft engine operation data disclosed by NASA. The results are compared with related references to verify the feasibility of the proposed method. Qualitative analysis shows the proposed method does not require the construction of an accurate physical model for the system. Quantitative analysis of historical monitoring data can accurately predict the remaining life in terms of sample similarity.

The remainder of this paper is organized as follows: the framework of RUL prediction based on TSBP and the trajectory extraction and similarity measurement methodology are described in detail in Section 2. The trajectory similarity measurement algorithm based on DTW is proposed in Section 3. The experimental analysis is given in Section 4. Finally, conclusions and future work are provided in Section 5.

2. RUL Prediction Based on TSBP

For most systems, degradation is irreversible. The characteristics observed in irreversible degradation may not be always monotonic, making it very difficult to parametrically build a model for the degradation process of system performance. Nevertheless, the degradation process can be represented by the trajectory of the measured states or characteristics. The useful life of an instance can, therefore, be estimated using the actual fault time of similar instances. The final RUL prediction is generated by assigning reasonable weights to several estimations of historical data. This is the basic idea of RUL prediction based on TSBP.

2.1. Framework of RUL Prediction Based on TSBP. TSBP is a nonparametric method particularly devised for RUL prediction. It extracts several degradation trajectories in the historical data of a system to generate a degradation model library. The similarity between models in the library can be evaluated by calculating the distance between two degradation trajectories. The known breakdown time of each degradation model is used to estimate the RUL of the system. The framework of RUL prediction based on TSBP is presented in Figure 1.

The RUL prediction based on TSBP mainly relies on two key techniques. One is degradation trajectory extraction, that is, using the degradation trajectories of training instances to build the instance/local models. The other is trajectory similarity measurement, which means to assess the training instances based on the degradation trajectory and the similarity between instance models and then obtain the RUL estimation from each instance model.

2.2. Degradation Trajectory Extraction. The performance state of a system may be represented with multiple measurable parameters, and the degradation state is irreversible. Extracting the degradation trajectories as an accurate reflection of the system performance state is vital to the RUL prediction based on TSBP. In practical RUL

prediction, attention is often paid to long-term system degradation, and any local variation of the degradation trajectory may be regarded as a disturbance or noise. The PCA is an unsupervised clustering technique and a common method for reducing the data dimensions. By reconstructing the projection of sample points by virtue of orthogonal transformation, the PCA can give the maximum variance vector of a given dimension in low-dimensional space. By abandoning the characteristic vectors at some minimum characteristic values, it obtains the integrated variable containing a large portion of information for the given dimension.

In practical applications, PCA can be conducted to reduce the dimensions of a characteristic vector and convert it into fewer principal components. Meanwhile, the PCA can eliminate the linear correlation between variables and inhibit the noise by integrating a number of the variables. All the monitored data of a system are generally normalized (with the mean value 0 and the variance 1) to lower the deviation that may be introduced by values that are too large in some of the monitored data. In PCA, the decomposition of the covariance matrix is conducted for the training and test data after normalization.

$$\mathbf{z} = (z_1, z_2, \dots, z_M)^T = V_M^T \cdot (y - \bar{y}), \quad (1)$$

where \bar{y} is the mean value of y ; V_M^T is the characteristic matrix sequentially formed by the characteristic vectors in correspondence with the first M characteristic values. These characteristics are uncorrelated with each other so that they are also known as orthogonal degradation characteristics. The number of characteristic vectors M is often determined by calculating its cumulative contribution $\theta = (\sum_{j=1}^p \lambda_j / \sum_{j=1}^m \lambda_j)$ and making it greater than a certain threshold, e.g., 90%.

It is assumed that the system has N -dimensional characteristic, $\mathbf{z} = (z_1, z_2, \dots, z_M)^T$ stands for its first M principal components ($M \leq N$), and $Z_I = \{z_1, z_2, \dots, z_I\}$ is the time series of these principal components. I denotes the time stamp of the latest measurement cycle. Let lG be a degradation trajectory model constructed using the time series lZ_I of the principal components based on the l^{th} training instance. Therefore, the degradation trajectory model of the system is represented by a function of principal components with time t as follows:

$${}^lG: \mathbf{z} = {}^l g(t) + \varepsilon, 0 \leq t \leq {}^l t_I, \quad (2)$$

where ε denotes the noise interference, which is often simulated by Gaussian noise.

In reference [34], four modeling methods for the degradation trajectory were compared and analyzed in terms of smoothing ability, training speed, and memory consumption, that is, exponential averaging, moving averaging, kernel regression, and relevance vector machine regression. The kernel regression was found to feature higher memory consumption but stronger smoothing ability, so it was then applied in a wider range. For this reason, kernel smoothing is employed to calculate the degradation trajectory model.

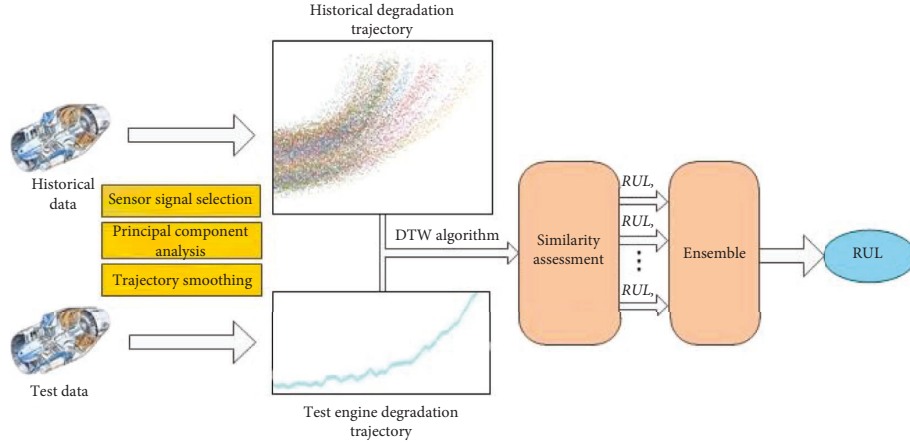


FIGURE 1: RUL prediction based on TSBP.

$$z(t) = \frac{\sum_{i=1}^E K(t, t_i) z_i}{\sum_{i=1}^E K(t, t_i)}, \quad (3)$$

where $K(\cdot)$ is the kernel function, and E denotes the end-of-life time stamp.

Among various kernels, the Gaussian kernel is the most widely applied and has been proved to provide more accurate results than other kernels [43]. In this paper, we compared four common kernel methods that are applicable and widely used, including the Gaussian kernel, Laplace kernel, polynomial kernel, and chi-squared kernel. Figure 2 shows the curve of HI prediction curve and corresponding fitting residual. It can be seen from the figure that the prediction curves of the polynomial kernel and chi-squared kernel are smoother than the others, while the variance of the prediction curve of the Laplace kernel is the smallest, and the performance of the Gaussian kernel is generally stable. Table 1 shows the comparison of the four kernels in terms of smoothing ability, training speed, evaluation speed, and storage consumption. It can be seen from Figure 2 and Table 1 that the polynomial kernel and chi-squared kernel prediction curves are the smoothest and have the fastest evaluation speed. However, it should be noted that the key disadvantage of these two methods is that the data are assumed to have a monotonous trend, that is, when the time series does not show an obvious trend, the algorithm may not converge. On the other hand, these two kernel methods ignore small fluctuations in the time series, which may correspond to the response of the system in a certain fault state. The Laplace kernel can reflect the small change of time series and has the minimum fitting error. However, this kernel method is not suitable for the later trajectory matching, since the excessively tortuous state change curve cannot well reflect the overall state of the system. Therefore, we applied the Gaussian kernel as the

fitting method of degradation curve, although this method has some disadvantages in memory consumption, which is expressed as follows:

$$K_G(x, y) = \exp\left(-\frac{\|x - y\|^2}{2\rho^2}\right), \quad (4)$$

where ρ is the parameter “kernel width,” which is often selected by cross validation.

2.3. Trajectory Similarity Measurement. Measuring the similarity between the degradation trajectories of a system is an important step in RUL prediction based on TSBP. For this purpose, a method is employed to quantitatively illustrate and describe the similarity between two degradation trajectories. Based on the similarity, the time series similar to the sample is subsequently discovered.

The trajectory similarity is generally measured by distance. The common measuring distances include Euclidean distance, Manhattan distance, Chebyshev distance, and Minkowski distance. Among them, Euclidean distance is more widely applied since it follows simple principles, is easy to understand, and gives a sufficient presentation of the differences between different points in a time series. To calculate the uncertainty distribution of RUL predictions at the same time, the average Euclidean distance between degradation trajectories is equal to the distance derived from the likelihood function to some extent. It is assumed that the system has M linearly independent principal components after PCA dimension reduction, and these components are subjected to the Gaussian distribution with the variance σ_m^2 . Hence, the similarity of a test sample Z_1 to the degradation model G can be defined as follows:

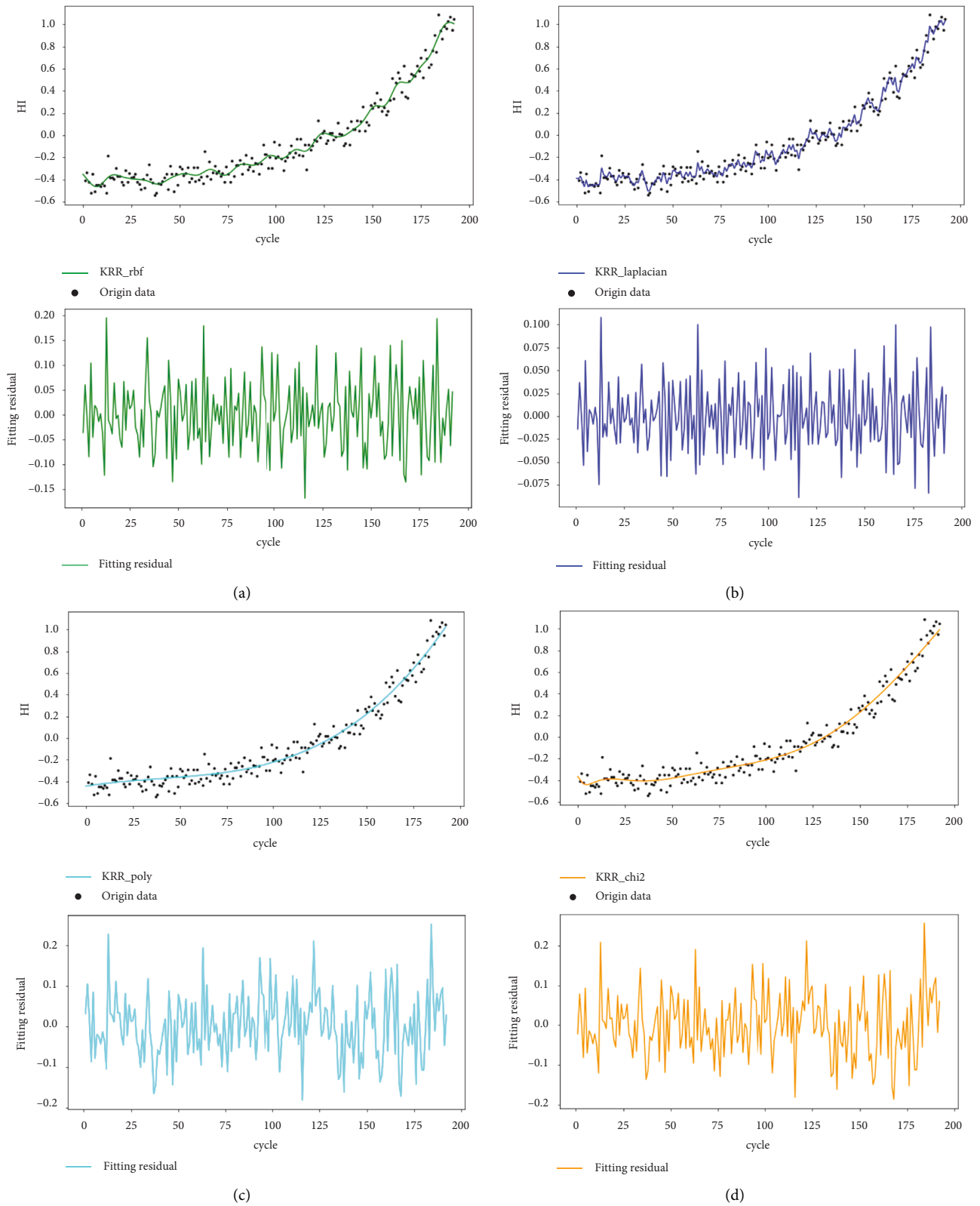


FIGURE 2: Kernel method comparison. (a) Gaussian kernel. (b) Laplace kernel. (c) Polynomial kernel. (d) Chi-squared kernel.

TABLE 1: Comparison of four data kernel methods.

| Kernel method | Smoothing power | Training speed | Evaluation speed | Storage consumption |
|--------------------|-----------------|----------------|------------------|---------------------|
| Gaussian kernel | Medium | Medium | Medium | High |
| Laplace kernel | Low | Slow | Slow | High |
| Polynomial kernel | Perfect | Fast | Fast | Low |
| Chi-squared kernel | High | Fast | Fast | Medium |

$$\begin{aligned}
L(Z_I | G) &= \prod_{i=1}^I \prod_{m=1}^M \left((2\pi\sigma_m^2)^{-(1/2)} \exp\left(-\frac{(z_{mi} - g_m(t_i))^2}{2\sigma_m^2}\right) \right) \\
&= \left(\prod_{m=1}^M (2\pi\sigma_m^2)^{-(1/2)} \right) \cdot \exp\left(-\sum_{i=1}^I \sum_{m=1}^M \frac{(z_{mi} - g_m(t_i))^2}{2\sigma_m^2}\right) \\
&= \left(\prod_{m=1}^M (2\pi\sigma_m^2)^{-(1/2)} \right) \cdot \exp\left(-\frac{1}{I} \sum_{i=1}^I \sum_{m=1}^M \frac{(z_{mi} - g_m(t_i))^2}{2\sigma_m^2}\right)^I.
\end{aligned} \tag{5}$$

The similarity between the test sample Z_I and the degradation model ${}^I G$ can be defined by the $(1/I)^{\text{th}}$ power of likelihood function as follows:

$$\begin{aligned}
{}^I S &:= (L(Z_I | G))^{(1/I)} \\
&= \prod_{m=1}^M (2\pi\sigma_m^2)^{-(1/2)} \cdot \exp\left(-\frac{1}{I} \sum_{i=1}^I \sum_{m=1}^M \frac{(z_{mi} - g_m(t_i))^2}{2\sigma_m^2}\right),
\end{aligned} \tag{6}$$

where $\prod_{m=1}^M (2\pi\sigma_m^2)^{-(1/2)}$ is a constant. The above equation can be further simplified into the following:

$${}^I S := \exp\left(-\frac{1}{I} \sum_{i=1}^I \sum_{m=1}^M \frac{(z_{mi} - g_m(t_i))^2}{2\sigma_m^2}\right). \tag{7}$$

Therefore, the square of the distance between degradation trajectories can be defined as

$${}^I D^2 := -\log {}^I S = \frac{1}{I} \sum_{i=1}^I \sum_{m=1}^M \frac{(z_{mi} - g_m(t_i))^2}{2\sigma_m^2}. \tag{8}$$

As shown in the above equation, the form of expression for the distance derived from the likelihood function is consistent with the calculation of the average Euclidean distance. The algorithms for measuring the similarity between the degradation trajectories of system performance and the similarity between the common trajectories based on distance are distinct for two reasons we mentioned in the introduction of this paper. Dynamic searching is carried out to measure the similarity between the trajectories at different lengths of a time series and at different degradation speeds.

3. Dynamic Time Warping Algorithm

The DTW is an algorithm based on the idea of dynamic warping. It can realize both ‘‘one-to-one’’ and ‘‘one-to-many’’ matching between data points. After overcoming the restrictions of length matching between data points, it can match the time series of different lengths.

3.1. Basic Principles of DTW Distance Algorithm. It is assumed that the perfect state of a system is the aligned state in the initial matching. Two time series are added. $O = \{o_1, o_2, o_3, \dots, o_n\}$ is the trajectory containing n pieces of data in the system degradation trajectory model library. $T = \{t_1, t_2, t_3, \dots, t_n\}$ includes the degradation trajectory points in the tested system. The distance between two points randomly selected in the interval from time series O to time series T should be calculated to match with the best path of the nearest distance. Euclidean distance is often used to calculate the distance between two points, i.e., $d(o_i, t_j) = \sqrt{(o_{ix} - t_{jx})^2 + (o_{iy} - t_{jy})^2}$, so as to construct a matrix F of the distance between O and T :

$$F = \begin{bmatrix} d(s_1, t_1) & \cdots & d(s_1, t_m) \\ \vdots & \vdots & \vdots \\ d(s_n, t_1) & \cdots & d(s_n, t_m) \end{bmatrix}. \tag{9}$$

The element $F(i, j)$ in the matrix F denotes the distance between o_i and t_j for the matching of two time series. The DTW is essentially a practice of optimization. It describes the correspondence between the degradation trajectories with a time warping function that satisfies certain conditions and determines the best path of the matrix F , which is the path for the minimum cumulative distance in the matching, as shown in Figure 3.

To find the best path of the distance matrix F , W is defined as the best path.

$$\begin{aligned}
W &= \{w_1, w_2, w_3, \dots, w_d, \dots, w_k\}, \\
k &\in \{\max(n, m), n + m - 1\},
\end{aligned} \tag{10}$$

where the k^{th} node of W is $w_k = (i, j)_k$. The mapping of time series O and T is defined to satisfy the following constraint conditions.

(1) *Boundary Conditions.* Path searching starts at $w_1 = (1, 1)$ and ends at $w_k = (m, n)$. (2) *Continuity.* Any two neighboring points of the best path, $w_{k-1} = (a, b)$ and $w_k =$

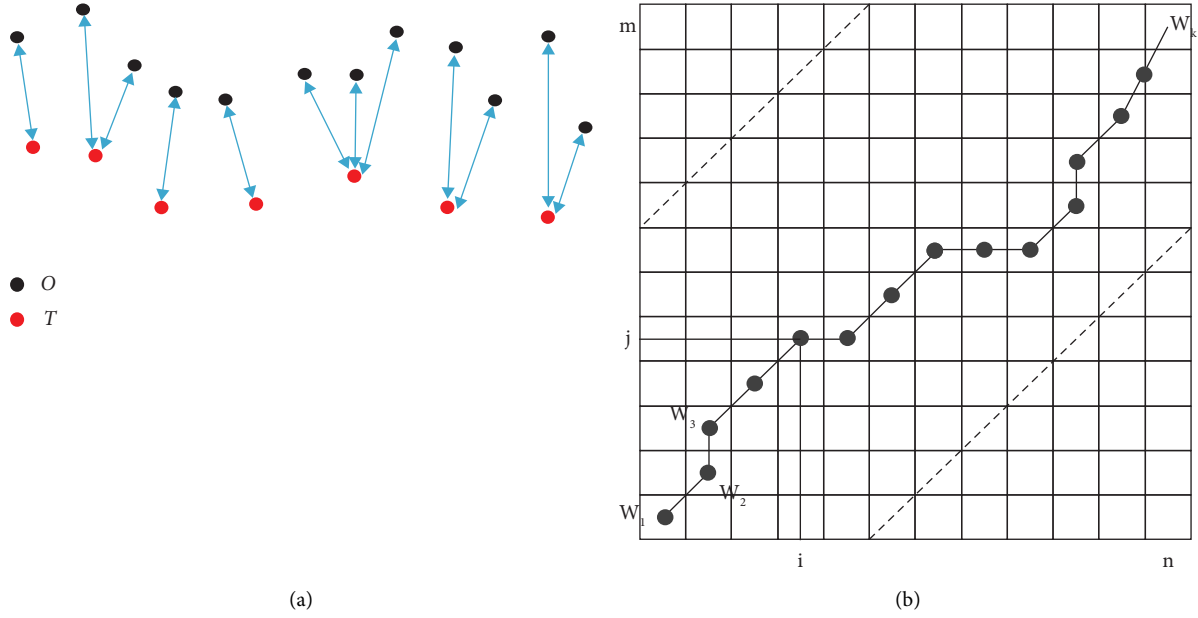


FIGURE 3: DTW track data relation and optimal path analysis. (a) Track data relation. (b) Optimal path analysis.

(c, d) , satisfy $0 \leq |c - a| \leq 1, 0 \leq |d - b| \leq 1$. (3) *Monotonicity*. If $w_k = (a, b)$, the next point $w_k = (c, d)$ needs to satisfy $c - a \geq 0, d - b \geq 0$. Therefore, the points on the best path W are monotonically upward.

Path searching is assumed to be at the point a_{ij} . According to the above constraint conditions, the next point in the path searching is above, on the right or upper right of the point as shown in Figure 4. The recurrence relation may be expressed as

$$w_{d+1} = w_d + \min[a_{(i+1)j}, a_{(i+1)(j+1)}, a_{i(j+1)}]. \quad (11)$$

The path with the minimum cumulative distance is selected, i.e., solving the DTW distance, by the following:

$$\begin{aligned} \text{DTW}(O, T) &= W_{\text{best}} \\ &= \min \left[\frac{1}{h} \sqrt{\sum_{i=1}^h w_i} \right], \end{aligned} \quad (12)$$

where h is the warping coefficient. The time series of different lengths are normalized.

The similarity between time series O and T can be defined by the sum of cumulative cost distances γ when the trajectory path is matched until the end. Any step in the cost distance γ is calculated as follows:

$$\gamma(i, j) = d(s_i, t_j) + \min \left[\begin{array}{l} \gamma(i-1, j-1), \\ \gamma(i-1, j), \gamma(i, j-1) \end{array} \right], \quad (13)$$

where $\gamma(0, 0) = 0, \gamma(i, 0) = \gamma(0, j) = \infty$.

The best path has the minimum cumulative cost distance γ . The similarity between time series O and T can be expressed as follows:

$$\text{DTW}(S, T) = \gamma(n, m). \quad (14)$$

3.2. Calculation Model of Degradation Trajectory DTW Distance. In the process of system degradation trajectory matching, system equipment may have different degradation trajectories and speeds. It is, therefore, difficult to compare and analyze the trajectories through the time series of fixed length, as shown in Figure 5. The DTW can lengthen and shorten the time series to effectively calculate the similarity among them, so that it is very suitable for comparing the degradation trajectories with time series of different lengths. The DTW can improve the similarity matching of degradation trajectories. Through PCA dimension reduction or health index (HI) extraction, the monitoring data of a system are reduced to one-dimensional data, and the indexes are extracted to reflect the system monitoring state. This can also reduce noise.

In practical applications, test samples and historical samples have different operation times at the initial stage (system operation state without wear). The length of sampling points for historical samples dynamically varies in the similarity analysis of the DTW distance. The number k of sampling points is searched to obtain the maximum similarity. In this case, the Euclidean distance and the likelihood function are adopted to estimate the DTW similarity as follows:

$${}^l D^2 = \min_{\tau} d^2(Z_I, {}^l G, k),$$

$$d^2(Z_I, {}^l G, k) = \min \left[\frac{1}{K} \sqrt{\sum_{i=1}^K \frac{1}{I} \sum_{i=1}^I \sum_{m=1}^M \frac{(z_{mi} - {}^l g_m(t_i + \tau))^2}{2\sigma_m^2}} \right]. \quad (15)$$

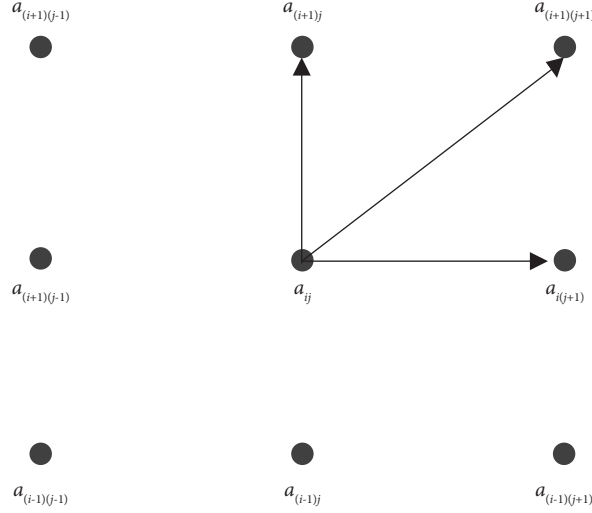


FIGURE 4: Optimal path search direction.

In the process of system performance degradation, the trajectory closer to the breakdown point should take up a larger portion of the measured similarity. Different weights should be assigned in the entire degradation trajectory. In the DTW calculation, the kernel density function based on the radial basis function (RBF) is employed to allocate the weights. The weights for different trajectory points are represented by the following:

$$v_i = \exp\left(-\frac{(t_i - t_I)^2}{2\eta^2}\right), \quad (16)$$

where t_i is the time of the i^{th} trajectory point for the test sample; η is the weight control coefficient. The optimal parameters are often obtained by virtue of cross validation. The procedure of the degradation trajectory similarity measurement based on DTW is given in Algorithm 1.

4. Verification of the Method

In this paper, the simulation datasets for aircraft engine performance degradation (run to failure) based on C-MAPSS are employed to verify the efficacy of the proposed method [44]. For this purpose, datasets disclosed by NASA are used to verify the RUL prediction algorithm based on the DTW distance. The datasets are first processed to reduce the multidimensional monitoring data into one-dimensional data. Subsequently, a DTW algorithm is employed to calculate the similarity between the performance degradation trajectory of the test engine and that of the engines in the sample library. After finding the samples with maximum similarity, weighting is carried out to determine the expected remaining useful life.

All simulation experiments were carried out in PyCharm 2021 (Community Edition) environment on a PC with an AMD Ryzen 7 3700X 8-core CPU and 16 GB memory.

4.1. Empirical Data Analysis. Figure 6 presents a sketch of an aircraft engine based on C-MAPSS, containing components

such as fan, combustion chamber, high/low-voltage compressor, turbine, and nozzle.

NASA disclosed five datasets. Each set contained over 100 engines. Each engine started in a healthy operational state. During their operation, different failures were randomly introduced to simulate system performance degradation. For the state of each engine, 24 variables were recorded, including three variables for operation setting and 21 variables for monitoring values, such as the number of work cycles, work environment parameters, and the monitoring data for each work cycle. White Gaussian noise was added to the monitoring data to simulate the influence of sensor noise. The data are used to simulate the actual system vividly in a highly credible manner.

The first of the five datasets disclosed by NASA was taken as an example to verify the method. Dataset 1 was divided into a training set and a test set. The training set consisted of the samples in the historical database, containing the data of 100 engines for their entire lives from normal operation to failure. The test set contained the data of test samples from their perfect states to failure.

4.2. Evaluation Indicators for Prediction Results. The common evaluation indicators for the RUL prediction results include mean absolute error (MAE), root mean square error, percentage error, and mean absolute percentage error (MAPE). In this paper, MAE and MAPE are taken as the evaluation indicators and calculated, respectively, by

$$\text{MAE} = \frac{1}{N_s} \sum_{j=1}^{N_s} |\widehat{RUL}_j - RUL_j|, \text{MAPE} = \frac{1}{N_s} \sum_{j=1}^{N_s} \left| \frac{\widehat{RUL}_j - RUL_j}{RUL_j} \right|, \quad (17)$$

where \widehat{RUL}_j and RUL_j are the predicted and actual values of RUL for the j^{th} test sample point, and N_s is the number of test samples. The smaller the MAE and MAPE are, the closer the predicted value given by the model is to the actual value, and the higher the prediction accuracy is.

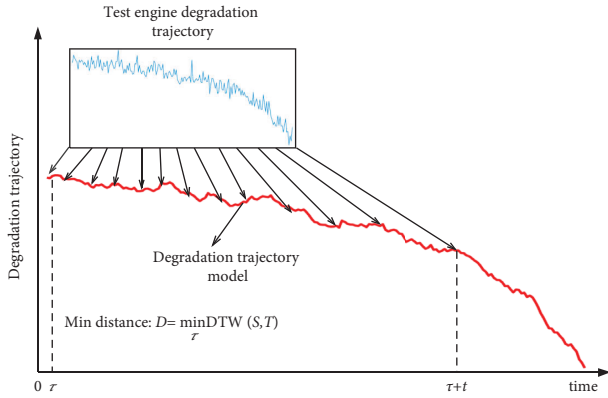


FIGURE 5: Comparison of degradation trajectories.

On the other hand, the higher RUL prediction causes more harm than the lower RUL prediction in practical application. Apart from MAPE, the segmented penalty

$$\text{Score}_{i,j} = \begin{cases} e^{-(q_{i,j}/13)} - 1, & q_{i,j} < 0, \\ e^{(q_{i,j}/10)} - 1, & q_{i,j} \geq 0, \end{cases}, \quad i = 1, \dots, N, \text{Score} = \sum_i \sum_j \text{Score}_{i,j}, \quad (18)$$

where $q_{i,j} = \text{RL}\hat{U}_j - \text{RUL}_j$ stands for the deviation of the RUL prediction for the i^{th} test sample at the time j from the actual value. The smaller the score, the more accurate the RUL prediction is.

In the model integration method, the upper and lower limits for the remaining useful life of similar samples are employed and weighted to determine the RUL prediction as follows:

$$\text{RUL}_p = r_1 \cdot \text{R}\hat{U}_{\max} + r_2 \cdot \text{R}\hat{U}_{\min}, \quad (19)$$

where $\text{R}\hat{U}_{\max}$ and $\text{R}\hat{U}_{\min}$ are the maximum and minimum predicted values in the similar sample set, and r_1 and r_2 are the corresponding weight coefficients.

4.3. Extraction of Aircraft Engine Performance Degradation Trajectories. First, the historical data of engines in the training test were analyzed. As shown in the distribution of data, some sensor signals were constant and did not vary with the operation of engine. Their data were removed to lower the linear correlation between data for the purpose of noise reduction. The variation trend of sensor signals was observed and analyzed, and then, the PCA was employed to reduce dimensions. The useful principal components are extracted as the source of data for the subsequent trajectory extraction. Table 2 lists the 14 sensor signals that were used for trajectory extraction.

Figure 7 presents the variation trend of 14 sensor signals of engine 1# in the training dataset within its life cycle. It must be noted that all the data had been normalized before analysis and varied between 0 and 1. As shown in the figure, the 14 sensor signals of the aircraft engine were monotonic

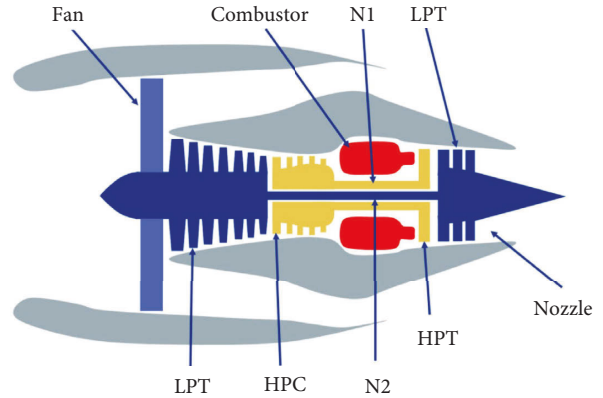


FIGURE 6: Structure diagram of C-MAPSS aeroengine.

factor put forward in [30] is also adopted and expressed as follows:

within the life cycle so that they could be used to extract the system performance degradation trajectories.

The PCA was adopted to reduce the dimensions of the 14-dimensional monitoring data. Only the first principal component was monotonic. As revealed in the test, it contained approximately 80% of the variance information. It is, therefore, adopted alone to evaluate the trajectory similarity. To extract the system's smooth degradation trajectories and achieve further noise reduction, two trajectory point smoothing methods were compared, that is, kernel ridge regression (KRR) and support vector regression (SVR). As revealed in Figure 8, the performance degradation trajectories extracted using KRR are smoother and can better reflect the actual state of system performance degradation. In contrast, the SVR curve dramatically fluctuates and deviates from the actual condition. Hence, KRR was adopted to extract the system performance degradation trajectories. An engine starts to operate in a healthy state so that it is illogical to have its remaining useful life showing a noticeable downtrend at this time. The remaining useful life segmentation model was, therefore, used. In other words, the remaining useful life was set as a constant at the initial stage, and the equipment degradation process was then divided into a constant stage and a linear decreasing stage. The remaining useful life at the initial stage was set to 125 [30].

4.4. DTW Distance Measurement Analysis. Figure 9 presents the results of the DTW distance measurement analysis for the first five engines in the test dataset to determine the best path. As shown in the figure, the optimal matched trajectory

Degradation trajectory similarity measurement based on DTW algorithm

Input: Test sample Z_I , degradation model lG

Output: Similarity between degradation trajectories $L(Z_I|{}^lG)$

Process:

- (1) Take out the N -dimensional measurable monitoring data of a system, reduce the dimensions through PCA after normalization to obtain the characteristic vectors of the first M principal components $\mathbf{z} = (z_1, z_2, \dots, z_M)^T$, and utilize kernel regression to obtain the trajectory model Z_I for the test sample.
- (2) Using the same parameters for normalization, PCA, and kernel regression, process all the historical samples to obtain the system degradation trajectory model library lG .
- (3) For $i = 1$ to l ($l = \text{number of trajectories in the model library}$).
- (4) For $j = 1$ to k ($k = \text{number of trajectory points in the historical samples}$).
- (5) Calculate $L_i(Z_I|G_j) = DTW(Z_I, {}^lG_j)$.
- (6) $L_i(Z_I|{}^lG) = \min(L_i(Z_I|{}^lG_j))$.
- (7) $L(Z_I|{}^lG) = \min(L_i(Z_I|{}^lG))$.

ALGORITHM 1: Trajectory similarity measurement algorithm.

TABLE 2: Engine sensor data description.

| Symbol | Description | Units |
|----------|--|--------------------|
| s_2 | Total temperature at low-pressure compressor outlet | $^{\circ}\text{C}$ |
| s_3 | Total temperature at high-pressure compressor outlet | $^{\circ}\text{C}$ |
| s_4 | Total temperature at low-pressure turbine outlet | $^{\circ}\text{C}$ |
| s_7 | Total pressure at high-pressure compressor outlet | kPa |
| s_8 | Physical fan speed | rpm |
| s_9 | Physical core speed | rpm |
| s_{11} | Static pressure at high-pressure compressor outlet | kPa |
| s_{12} | Ratio of fuel flow to Ps30 | — |
| s_{13} | Corrected fan speed | rpm |
| s_{14} | Corrected core speed | rpm |
| s_{15} | Bypass ratio | — |
| s_{17} | Bleed enthalpy | — |
| s_{20} | High-pressure turbine coolant bleed | kg/s |
| s_{21} | Low-pressure turbine coolant bleed | kg/s |

based on DTW measurement is basically consistent. The similarity between DTW distances is generally between 0.1 and 0.2.

4.5. Analysis of RUL Prediction Results. Figure 10 shows the comparison of the predicted and actual remaining useful lives. The predicted value is very close to the actual value so that the prediction is satisfactory.

Following the practice in [35, 36], the prediction results are divided into three ranges including advanced prediction, timely prediction, and delayed prediction. Among them, timely prediction means that the predicted value is between -10 and 13 . Table 3 presents a comparison of the prediction results obtained in this paper in terms of specific indicators with other models including reduced kernel recursive least squares (reduced kernel RLS), deep belief network-hidden Markov model (DBN-HMM), and double-layer random forest (double-layer RF).

The comparison reveals that the prediction results obtained in this paper are relatively better in terms of evaluation indicators. Evaluation indicators are vital to the assessment of an algorithm. It must be noted that different harms of advanced prediction and delayed prediction are taken into account in the development of the indicator

“score.” Therefore, it is more important than other evaluation indicators when a dataset based on C-MAPSS is used in the RUL prediction. The smaller the score, the higher the accuracy of prediction. The score obtained with the algorithm is lower than that in [35] by 39%. Moreover, Table 1 shows that the indicator MAPE for the prediction results obtained in this paper is higher than that in [35] by 8.15%. It is believed that this must be attributed to the tendency of MAPE to predict lower than the actual value. In other words, MAPE imposes a higher penalty on advanced prediction. In a future study, attention may be paid to adjusting the focus on the hyperparameter optimization and the remaining life calculation model after trajectory similarity matching. Figures 10 and 11 present the prediction error between the actual RUL of the engines and the prediction results based on the model we proposed. Based on the prediction error histogram in Figure 11, the prediction errors are basically subjected to normal distribution and are around 0, so that the prediction results are highly credible. Based on the scatter plot of prediction errors in Figure 12, the prediction error for engines with remaining useful life cycles of less than 60 is obviously lower than that for those with cycles between 60 and 130. Higher prediction errors are generally seen in cycles between 60 and 130. The larger error must be caused by the

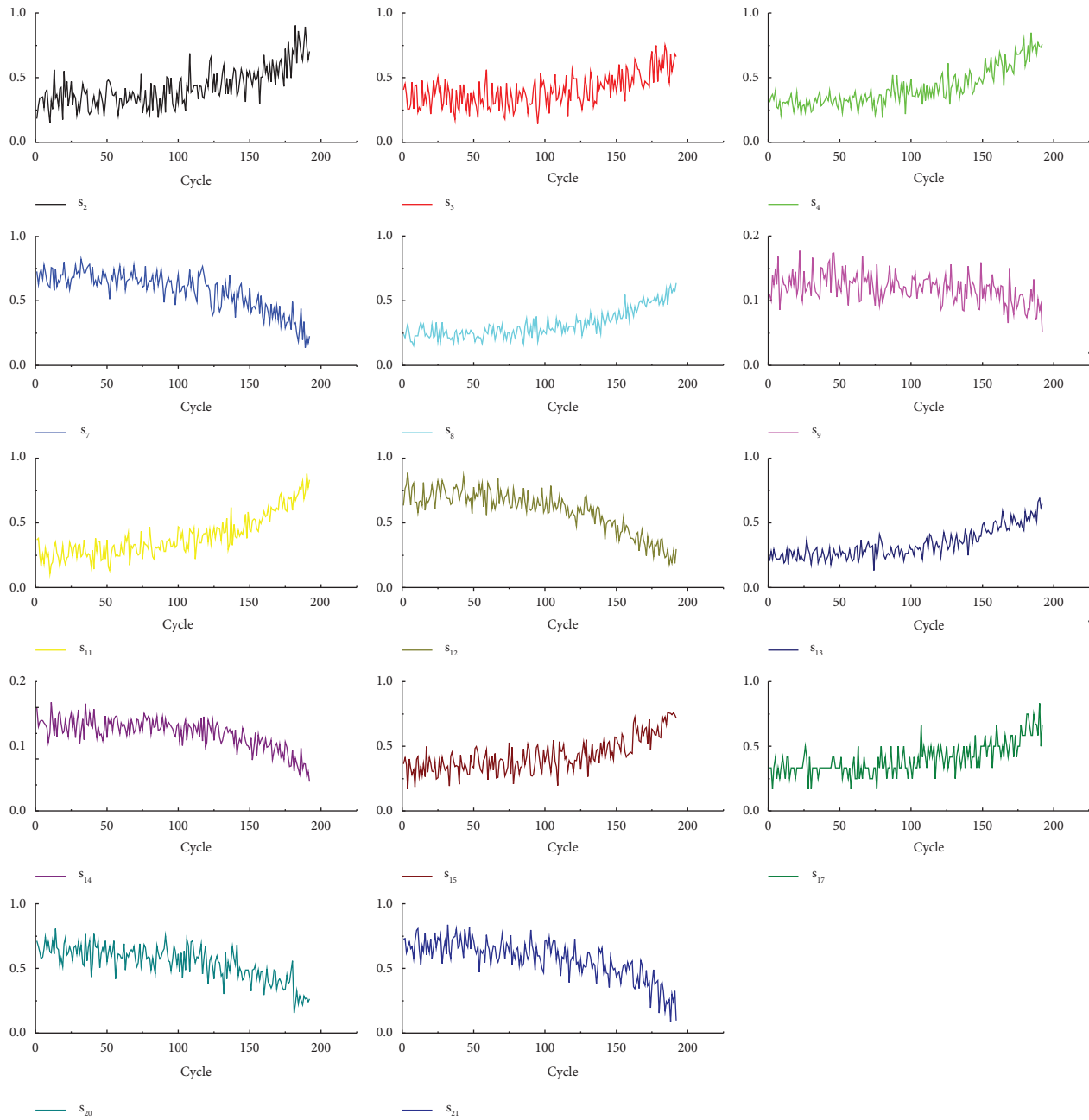


FIGURE 7: Trend example engine sensor data.

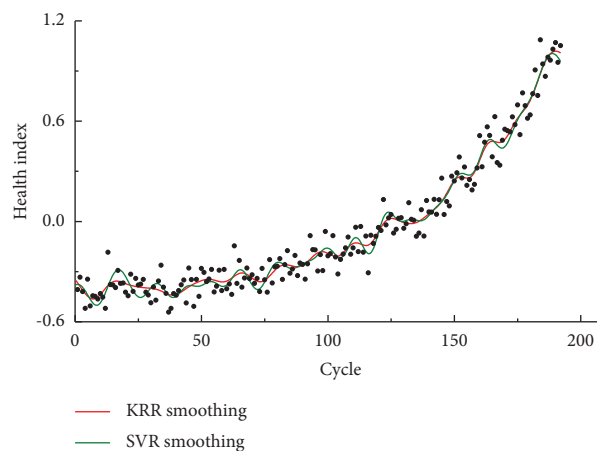


FIGURE 8: Comparison of SVR and KRR performance.

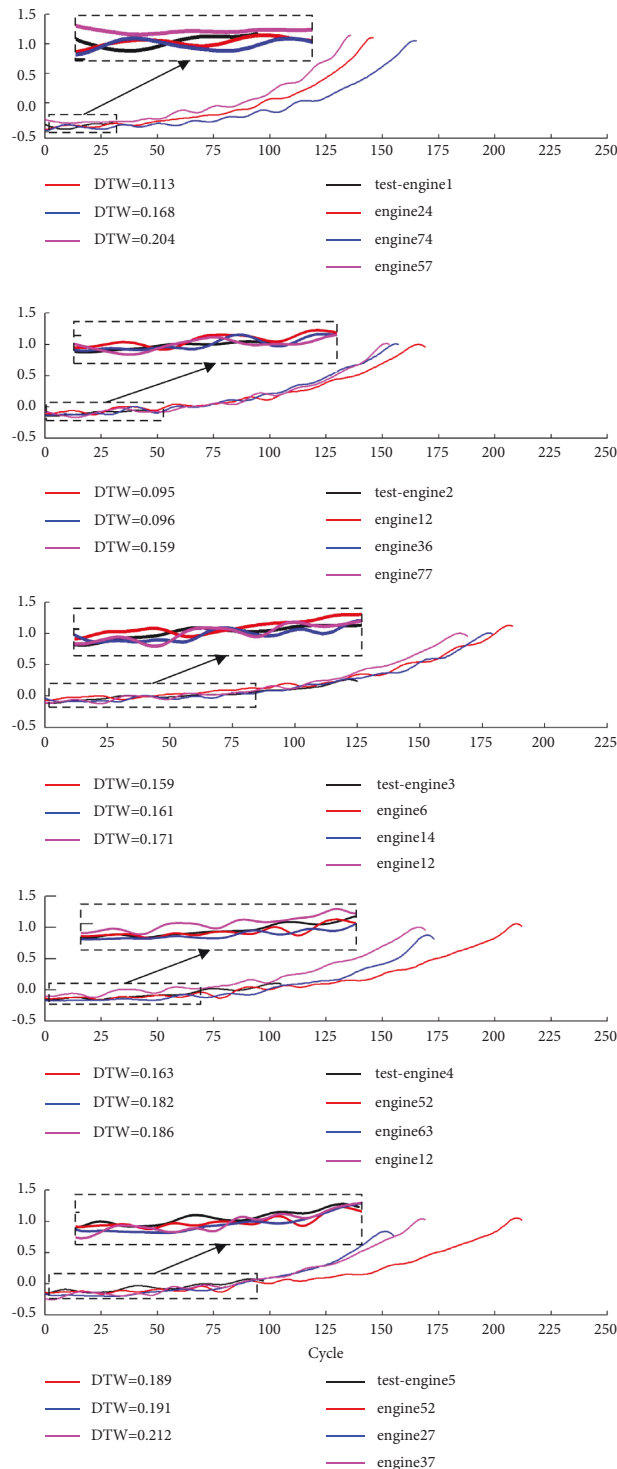


FIGURE 9: DTW similarity matching of test engine trajectory.

longer remaining useful life of the system, which leads to less historical data and a shorter degradation trajectory for DTW distance matching.

The C-MAPSS dataset contains two failure modes. Before modeling, most algorithms need the classification algorithm to classify the datasets in terms of failure mode. Subsequently, a suitable global model can be constructed. The algorithm in this paper does not simply use the failure

mode but integrates the information of different failure modes to build a unified degradation trajectory model. Indeed, this is more consistent with actual conditions. A system may fail for various reasons, and a hybrid failure mode is very often encountered in practice. Therefore, it is very difficult to accurately classify the reasons for system failure in advance. The above test process and results have also verified this feature of the algorithm.

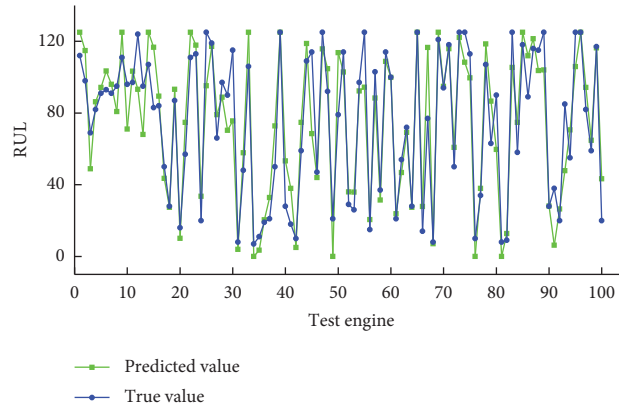


FIGURE 10: Comparison of RUL predictions.

TABLE 3: Comparison of prediction results.

| Method | Score | MAPE | MAE | Timely | Advance | Delay |
|-----------------------------|------------|--------------|--------------|-----------|-----------|-----------|
| DBN-HMM [45] | — | — | 24.54 | 51 | 31 | 18 |
| Reduced kernel RLS [36] | 612 | — | — | 40 | 34 | 26 |
| Double-layer RF [35] | 1567 | 24.05 | — | 50 | 27 | 23 |
| Degradation similarity [35] | 682 | 18.05 | — | 63 | 10 | 27 |
| Proposed method | 417 | 26.2 | 12.74 | 58 | 22 | 20 |

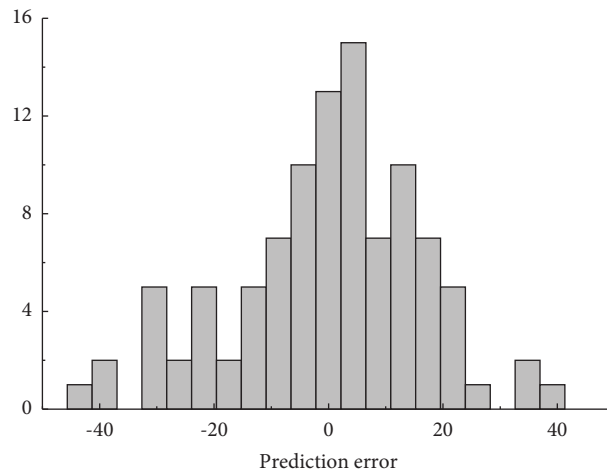


FIGURE 11: Histogram distribution of prediction error.

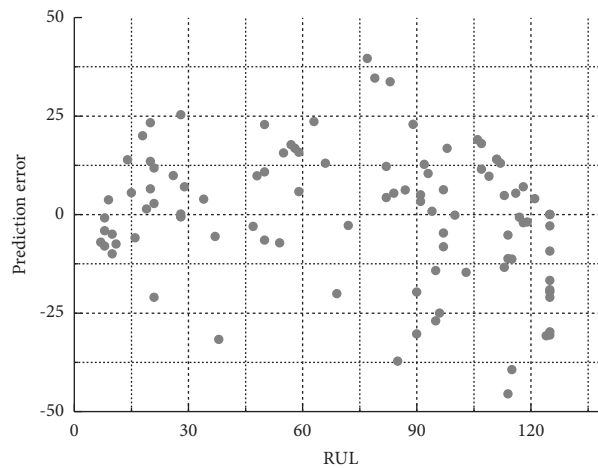


FIGURE 12: Scatter distribution of prediction error.

5. Conclusions

A comparative analysis method of degradation trajectory based on dynamic time warping (DTW) is put forward to estimate the remaining useful life of a system. The principal component analysis is carried out for dimension and noise reduction, and the characteristics of a system degradation trajectory are then extracted. Kernel regression is employed for the smoothing and further noise reduction in degradation trajectories. The RUL prediction is conducted through the remaining life weighting of similar trajectories. In the end, the aircraft engine data disclosed by NASA are utilized to verify the RUL prediction based on DTW. The results are compared with those of the latest references to verify the feasibility of the proposed method. Qualitative analysis shows the proposed method does not require the construction of an accurate physical model for the system. Qualitative and quantitative analyses of historical monitoring data can accurately predict the remaining life in terms of sample similarity.

The RUL prediction based on DTW may bring optimal results compared to similar methods, but it can still be further improved. For instance, in the process of practical application, it is difficult to collect sufficient training data like the C-MAPSS dataset. In the case of small samples, the matching of degradation trajectory may be inaccurate; thus, the RUL may not be accurately predicted. On the other hand, the prediction method should be adjusted appropriately when multiple failures occur concurrently in the system. A feasible way to solve the above problems is to introduce domain knowledge, induce the possible fault types and multiple fault combination modes of the system, and conduct classification modeling and prediction according to the characteristics of sensor signals.

The follow-up research will mainly focus on the research and verification of RUL prediction methods based on real engine operation data. In the future, the engine degradation mechanism and RUL prediction will be studied and verified by using the real data accumulated during the engine operation, combined with engine vibration, oil analysis, etc., to improve the RUL prediction accuracy and increase the engineering practicability of the prediction method.

Data Availability

The data used to support the findings of this study are openly available at https://github.com/huanglinxixi/DTW_RUL_Trajectory.git.

Conflicts of Interest

The authors declare that they have no conflicts of interest.

Acknowledgments

This work was financially supported by the National Nature Science Foundation of China (51879269) and the Naval

Equipment Research Foundation of China (HJ20191C030583).

References

- [1] E. Zio, "Prognostics and Health Management (PHM): where are we and where do we (need to) go in theory and practice," *Reliability Engineering & System Safety*, vol. 218, Article ID 108119, 2022.
- [2] T. Sutharssan, D. Montalvao, Y. K. Chen, W. C. Wang, C. Pisac, and H. Elemara, "A review on prognostics and health monitoring of proton exchange membrane fuel cell," *Renewable and Sustainable Energy Reviews*, vol. 75, pp. 440–450, 2017.
- [3] N. Li, Y. Lei, T. Yan, N. Li, and T. Han, "A Wiener-process-model-based method for remaining useful life prediction considering Unit-to-Unit variability," *IEEE Transactions on Industrial Electronics*, vol. 66, no. 3, pp. 2092–2101, 2019.
- [4] J. Wang, R. X. Gao, Z. Yuan, Z. Fan, and L. Zhang, "A joint particle filter and expectation maximization approach to machine condition prognosis," *Journal of Intelligent Manufacturing*, vol. 30, no. 2, pp. 605–621, 2019.
- [5] Y. Cheng, Z. Wang, W. Zhang, and G. Huang, "Particle swarm optimization algorithm to solve the deconvolution problem for rolling element bearing fault diagnosis," *ISA Transactions*, vol. 90, pp. 244–267, 2019.
- [6] Y. Deng, A. D. Bucchianico, and M. Pechenizkiy, "Controlling the accuracy and uncertainty trade-off in RUL prediction with a surrogate Wiener propagation model," *Reliability Engineering & System Safety*, vol. 196, Article ID 106727, 2020.
- [7] Y. Wang, Z. Chen, Y. Zhang, X. Li, and Z. Li, "Remaining useful life prediction of rolling bearings based on the three-parameter Weibull distribution proportional hazards model," *Insight - Non-Destructive Testing and Condition Monitoring*, vol. 62, no. 12, pp. 710–718, 2020.
- [8] W. Yu, W. Tu, I. Y. Kim, and C. Mechefske, "A nonlinear-drift-driven Wiener process model for remaining useful life estimation considering three sources of variability," *Reliability Engineering & System Safety*, vol. 212, Article ID 107631, 2021.
- [9] M. H. Moulahi and F. Ben Hmida, "Using extended Kalman filter for failure detection and prognostic of degradation process in feedback control system," *Proceedings of the Institution of Mechanical Engineers - Part I: Journal of Systems & Control Engineering*, vol. 236, no. 1, pp. 182–199, 2021.
- [10] H. Zhao, H. Liu, Y. Jin, X. Dang, and W. Deng, "Feature extraction for data-driven remaining useful life prediction of rolling bearings," *IEEE Transactions on Instrumentation and Measurement*, vol. 70, pp. 1–10, 2021.
- [11] X. Shu, S. Shen, J. Shen et al., "State of health prediction of lithium-ion batteries based on machine learning: Advances and perspectives," *iScience*, vol. 24, no. 11, Article ID 103265, 2021.
- [12] Y. Li, X. Huang, C. Zhao, and P. Ding, "A Novel Remaining Useful Life Prediction Method Based on Multi-Support Vector Regression Fusion and Adaptive Weight Updating," *ISA Transactions*, 2022.
- [13] J. Ma, Y. Wang, X. Niu, S. Jiang, and Z. Liu, "A Comparative Study of Mutual Information-Based Input Variable Selection Strategies for the Displacement Prediction of Seepage-Driven Landslides Using Optimized Support Vector Regression," *Stochastic Environmental Research and Risk Assessment*, vol. 36, pp. 1–21, 2022.
- [14] L. Huang, Li Gong, W. Jiang, and K. Wang, "Remaining useful life prediction based on multi-source information fusion and

- HMM,” *Systems Engineering and Electronics*, vol. 44, no. 5, pp. 1747–1756, 2022.
- [15] S. Jia, B. Ma, W. Guo, and Z. S. Li, “A sample entropy based prognostics method for lithium-ion batteries using relevance vector machine,” *Journal of Manufacturing Systems*, vol. 61, pp. 773–781, 2021.
 - [16] M. Tanwar and N. Raghavan, “Lubricating oil remaining useful life prediction using multi-Output Gaussian process regression,” *IEEE Access*, vol. 8, Article ID 128897, 2020.
 - [17] P. Xia, Y. Huang, P. Li, C. Liu, and L. Shi, “Fault knowledge transfer Assisted ensemble method for remaining useful life prediction,” *IEEE Transactions on Industrial Informatics*, vol. 18, no. 3, pp. 1758–1769, 2022.
 - [18] J. Ma, X. Liu, X. Niu et al., “Forecasting of landslide displacement using a Probability-Scheme combination ensemble prediction technique,” *International Journal of Environmental Research and Public Health*, vol. 17, no. 13, p. 4788, 2020.
 - [19] J. Ma, H. Tang, X. Hu et al., “Identification of causal factors for the Majiagou landslide using modern data mining methods,” *Landslides*, vol. 14, no. 1, pp. 311–322, 2017.
 - [20] L. Zhang, J. Lin, B. Liu, Z. Zhang, X. Yan, and M. Wei, “A review on deep learning applications in prognostics and health management,” *IEEE Access*, vol. 7, Article ID 162415, 2019.
 - [21] S. Wang, S. Jin, D. Bai, Y. Fan, H. Shi, and C. Fernandez, “A critical review of improved deep learning methods for the remaining useful life prediction of lithium-ion batteries,” *Energy Reports*, vol. 7, pp. 5562–5574, 2021.
 - [22] P. Aivaliotis, K. Georgoulas, and G. Chryssoulouris, “The use of Digital Twin for predictive maintenance in manufacturing,” *International Journal of Computer Integrated Manufacturing*, vol. 32, no. 11, pp. 1067–1080, 2019.
 - [23] B. He, L. Liu, and D. Zhang, “Digital twin-driven remaining useful life prediction for gear performance degradation: a review,” *Journal of Computing and Information Science in Engineering*, vol. 21, no. 3, Article ID 30801, 2021.
 - [24] S. Meraghni, L. S. Terrissa, M. Yue, J. Ma, S. Jemei, and N. Zerhouni, “A data-driven digital-twin prognostics method for proton exchange membrane fuel cell remaining useful life prediction,” *International Journal of Hydrogen Energy*, vol. 46, no. 2, pp. 2555–2564, 2021.
 - [25] M. Xiong, H. Wang, Q. Fu, and Y. Xu, “Digital twin-driven aero-engine intelligent predictive maintenance,” *International Journal of Advanced Manufacturing Technology*, vol. 114, no. 11–12, pp. 3751–3761, 2021.
 - [26] Y. Lei, N. Li, L. Guo, N. Li, T. Yan, and J. Lin, “Machinery health prognostics: a systematic review from data acquisition to RUL prediction,” *Mechanical Systems and Signal Processing*, vol. 104, pp. 799–834, 2018.
 - [27] Y. Hu, X. Miao, Y. Si, E. Pan, and E. Zio, “Prognostics and health management: a review from the perspectives of design, development and decision,” *Reliability Engineering & System Safety*, vol. 217, Article ID 108063, 2022.
 - [28] D. W. Aha, D. Kibler, and M. K. Albert, “Instance-based learning algorithms,” *Machine Learning*, vol. 6, no. 1, pp. 37–66, 1991.
 - [29] R. Liu, B. Yang, E. Zio, and X. Chen, “Artificial intelligence for fault diagnosis of rotating machinery: a review,” *Mechanical Systems and Signal Processing*, vol. 108, pp. 33–47, 2018.
 - [30] T. Wang, Y. Jianbo, D. Siegel, and J. Lee, “A Similarity-Based Prognostics Approach for Remaining Useful Life Estimation of Engineered Systems,” in *Proceedings of the 2008 International Conference on Prognostics and Health Management*, pp. 1–6, Denver, CO, USA, October 2008.
 - [31] Y. Liu, L. Li, S. Zhao, and S. Song, “A global surrogate model technique based on principal component analysis and Kriging for uncertainty propagation of dynamic systems,” *Reliability Engineering & System Safety*, vol. 207, Article ID 107365, 2021.
 - [32] D. Huang, L. Ke, M. Lin, and G. Sun, “A new fault diagnosis approach for bearing based on multi-scale entropy of the optimized VMD,” *Control and Decision*, vol. 35, no. 7, pp. 1631–1638, 2020.
 - [33] W. Yonghe, W. Liu, Y. Yang, and J. Su, “A model of bearing fault diagnosis based on LLE and its improved distance algorithm,” *Modular Mach Tool Autom Mach Technol*, no. 7, pp. 73–77, 2018.
 - [34] T. Wang, “Trajectory similarity based prediction for remaining useful life estimation,” Ph.D. Thesis, University of Cincinnati, Cincinnati, OH, USA, 2010.
 - [35] Y. Zhang, C. Wang, N. Lu, and B. Jiang, “Remaining useful life prediction for aero-engine based on the similarity of degradation characteristics,” *Systems Engineering and Electronics*, vol. 41, no. 6, pp. 1414–1421, 2019.
 - [36] H. Zhou, J. Huang, and F. Lu, “Reduced kernel recursive least squares algorithm for aero-engine degradation prediction,” *Mechanical Systems and Signal Processing*, vol. 95, pp. 446–467, 2017.
 - [37] D. J. Berndt and J. Clifford, “Using dynamic time warping to find patterns in time series,” in *Proceedings of the 3rd International Conference on Knowledge Discovery and Data Mining*, vol. 10, no. 16, pp. 359–370, Seattle, WA, July 1994.
 - [38] D. Ram, A. Asaei, and H. Bourlard, “Sparse Subspace modeling for Query by example Spoken term detection,” *IEEE/ACM Transactions on Audio, Speech, and Language Processing*, vol. 26, no. 6, pp. 1130–1143, 2018.
 - [39] M. Kowdiki and A. Khaparde, “Automatic hand gesture recognition using hybrid meta-heuristic-based feature selection and classification with Dynamic Time Warping,” *Computer Science Review*, vol. 39, Article ID 100320, 2021.
 - [40] A. Ismail, S. Abdlerazek, and I. M. El-Henawy, “Development of Smart Healthcare system based on speech recognition using support vector machine and dynamic time warping,” *Sustainability*, vol. 12, no. 6, pp. 2403–2415, 2020.
 - [41] Z. Zheng, M. Zhou, Y. Chen et al., “A Fused method of machine learning and dynamic time warping for road anomalies detection,” *IEEE Transactions on Intelligent Transportation Systems*, vol. 23, no. 2, pp. 827–839, 2022.
 - [42] R. Yang, D. Zhang, Z. Li, K. Yang, S. Mo, and L. Li, “mechanical fault diagnostics of power transformer on-Load Tap Changers using dynamic time warping,” *IEEE Transactions on Instrumentation and Measurement*, vol. 68, no. 9, pp. 3119–3127, 2019.
 - [43] J. Ma, D. Xia, H. Guo et al., “Metaheuristic-based support vector regression for landslide displacement prediction: a comparative study,” *Landslides*, vol. 19, no. 10, pp. 2489–2511, 2022.
 - [44] A. Saxena, K. Goebel, D. Simon, and N. Eklund, “Damage propagation modeling for aircraft engine run-to-failure simulation,” in *Proceedings of the 2008 International Conference on Prognostics and Health Management*, pp. 1–9, Denver, CO, USA, October 2008.
 - [45] K. X. Peng, Y. T. Pi, and R. H. Jiao, “Health indicator construction and remaining useful life prediction for aircraft engine,” *Control Theory & Applications*, vol. 37, no. 4, pp. 713–720, 2020.